

# Analysis of Strength Test Results — Pnyang Formation Rocks — Papua New Guinea

G. MOSTYN

Senior Geotechnical Engineer, Dames & Moore, Sydney

and

A.J. FERGUSON

Geotechnical Engineer, Dames & Moore, Sydney

**SUMMARY** A large suite of classification and strength test results on samples obtained from the Pnyang Formation is presented. The Pnyang Formation is a poorly consolidated finely bedded grey calcareous mudstone of Middle Miocene Age, it is thus typical of many soft rocks. The individual test data are presented in graphical form and where possible relationships between parameters are established. A strong relationship is derived between dry density and effective strength. The paper both provides a data base and illustrates appropriate statistical techniques.

## 1 PROJECT BACKGROUND

The Ok Tedi gold and copper mine is located in the Star Mountains, Papua New Guinea. The mine is being developed by Ok Tedi Mining Ltd, a consortium involving the Papua New Guinea Government, Australian, U.S. and German interests. Bechtel-MKI (a joint venture) is responsible for the design and construction of Stage I of the mine infrastructure. The estimated capital cost of this development is approximately US \$800 million.

Dames & Moore were awarded a site investigation contract in late 1981 to provide geotechnical consultancy services and data collection for construction of the development. The investigation continued throughout 1982 and employed six drilling rigs for twelve months.

As part of this contract an extensive programme of laboratory tests was completed on the samples of soil and rock obtained during the drilling. The programme was specified by the design engineers and included index and classification tests and numerous undrained and effective strength tests. The tests were completed in on-site laboratories and central laboratories in both Sydney and San Francisco.

The mine site is situated in one of the most remote areas of the world, see Figure 1. The topography is extremely rugged and supplies, personnel, core and drill rigs were moved by helicopter during most of the site investigation.

The high ranges of the northern part of the mine site are flanked to the south by ridge and ravine landforms, with deeply incised valleys. The Hindenberg Wall, approximately 10 km to the north of the mine site area comprises an almost vertical limestone scarp up to 1000 metres high.

## 2 GEOLOGY

The regional geology is described in the report accompanying the geological map of the area (Arnold et al, 1979) and is summarised below. The Ok Tedi mine pit is to be located at Mount Fubilan, within the Ok Tedi Complex, an intrusion containing high level porphyry stocks of Upper Miocene to Pleistocene Age.

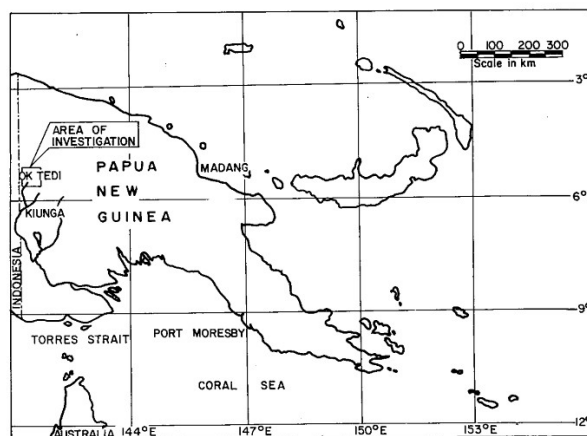


Figure 1 Location of project

The sediments in the mine area through which the Ok Tedi Complex intrudes comprise, in ascending order:

- o the Upper Jurassic to Upper Cretaceous Ieru Formation;
- o the Late Eocene to Middle Miocene Darai Limestone;
- o the Middle Miocene Pnyang Formation (which forms the subject of this paper);
- o the Upper Miocene to Pliocene Birim Formation, and;
- o surficial deposits of colluvium and alluvium.

The Ieru Formation consists predominantly of black mudstone near its base and of glauconitic sandstone and siltstone and grey mudstone over its upper section. The formation is up to 1,500 metres in stratigraphic thickness. Disconformably overlying the Ieru is the Darai Limestone which comprises monotonous massive foraminiferal lime packstone, mudstone and wackestone. This unit comprises the almost vertical scarps of the Hindenberg Wall and is itself up to 1,500 metres thick.

The Pnyang Formation comprises mainly calcareous mudstones and siltstones, with some limestone and sandstone horizons. The unit was deposited in a shallow marine environment, with non-marine conditions affecting some areas for short periods. The



stratigraphic thickness of the formation is approximately 1,000 metres. Complex folding and faulting associated with the Ok Tedi Complex has caused several sheared and weakened zones within the unit.

The colluvial deposits include extensive aprons derived from debris flows formed by failures along the Darai Limestone scarps. Partly lithified alluvium forms dissected raised terraces in several areas, particularly along the Ok Tedi river.

### 3 TESTING PROGRAMME

The testing programme considered herein was carried out as a part of the site investigation for one of the dams associated with the project. The data and statistical correlations contained herein are presented both as a "model case" for statistical analysis of a large test data base, and to record relationships derived from this data.

Similar correlations of strength and other material properties have been derived previously by others. Mayne (1980) investigated undrained strength in clay soils. Everitt and Goldfinch (1983) considered the shear strength of clay gouge in sedimentary rocks. Others (Chui and Johnston, 1983; Onodera and Duangdeun, 1981 and Saint Simon et al, 1979) evaluated strength characteristics of soft rocks, while Mandzic (1979) and Smorodinov et al (1971) investigated hard rocks. While the above referenced papers were based on different suites of tests, several relationships similar to the ones derived herein were presented.

### 4 DESCRIPTIVE AND INDEX PROPERTIES

The descriptive and index testing carried out comprised visual description, moisture content, dry density, and plastic and liquid limit determination. Most rock samples from the shear zones or the upper weathered zone exhibited sufficient plasticity to allow plastic limit testing to be carried out. Some tests were also performed on stronger samples by grinding with a mortar and pestle.

Summary statistics for the descriptive and index tests completed as part of the test programme are included in Table I. All samples were obtained from depths between 1.2 and 44 metres. These statistics are as would be expected except for the relatively high mean and maximum densities. The

scatter of moisture content ( $\omega_n$ ), dry density ( $\rho_d$ ) and liquidity index ( $I_L$ ) with depth is shown on Figure 2. As would be expected, density increases significantly with depth, whilst moisture content decreases significantly. A trend indicating a small decrease in liquidity index with depth is apparent, but this is overshadowed by the low number and inherent scatter of the test results. Regression analyses were performed to quantify these trends, the relationships derived are:

$$\omega_n = 33.4 - 14.7 \log(z)\% \quad (1)$$

with a standard error of 4.8%  
and r squared of 0.488

$$\rho_d = 1.36 + 0.50 \log(z) \text{ tm}^{-3} \quad (2)$$

with a standard error of 0.17  $\text{tm}^{-3}$   
and r squared of 0.479

The extremely high rainfall and heavy vegetation cover resulted in a shallow water table at most drill sites. The plot of moisture content versus dry density is shown on Figure 3 and indicates that the sample test results are scattered about the zero air void line for a particle density of 3.0  $\text{tm}^{-3}$ . In fact, about eight percent of the 269 results gave calculated saturations in excess of one hundred percent. This result is a little surprising in view of the following facts:

- o all tests were carried out with strict adherence to recognised laboratory practice and relevant standards;
- o tests were completed by several technicians both in site laboratories and in laboratories in Sydney and San Francisco. No systematic differences were detected between the results from the various laboratories.

We have concluded that the test results indicating oversaturation are due to:

- o many of the samples had a large pyrite content, in fact pyrite crystals could be seen clearly;
- o inherent variation between the subsamples tested for moisture and density;
- o errors inherent in density test procedures, in particular in the volume measurement for cored samples;
- o some variation in particle density. Note that the value adopted is very high, but is considered reasonable in view of the following.

TABLE I  
SUMMARY STATISTICS OF INDEX TESTS

Parameter	Symbol	Unit	No. of test results	Mean	Standard deviation	Minimum	Maximum
Moisture content	$\omega$	%	274	17.4	6.6	7.2	55
Dry density	$\rho_d$	$\text{tm}^{-3}$	269	1.90	0.23	1.09	2.56
Total density	$\rho_t$	$\text{tm}^{-3}$	269	2.22	0.18	1.68	2.80
Plasticity index	$I_p$	%	58	17.5	6.9	2.5	35
Liquid limit	$\omega_l$	%	58	37.5	7.9	22	65
Deviation from A-line	-	%	58	4.7	2.9	-4.0	9.4
Liquidity Index	$I_L$	-	53	-0.08	0.60	-2.52	2.36
Minimum particle density for saturation	-	$\text{tm}^{-3}$	269	2.79	0.20	2.10	3.74



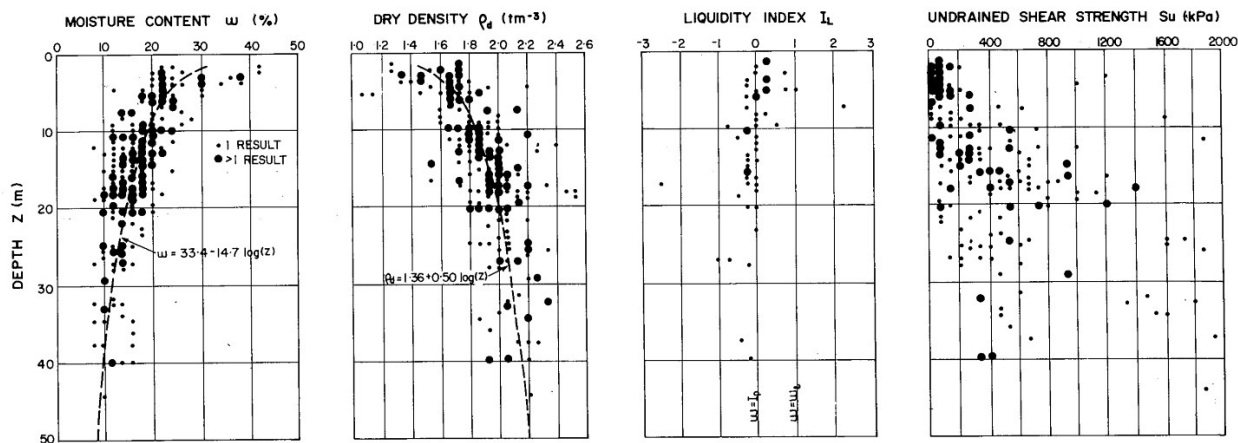


Figure 2 Scatter of moisture content, dry density, liquidity index and undrained Shear Strength with Depth.

The minimum possible particle density was calculated for each moisture content/dry density pair, the statistics of this parameter are also given in Table I. The mean minimum possible particle density is  $2.79 \text{ tm}^{-3}$  and the actual mean particle density would be higher due to the fact that some samples were definitely not saturated.

The Atterberg limit test results are plotted on Figure 4, the deviation of the plasticity index from the A-line is shown on the lower plot. The test results show that the rock is a clay of low plasticity when remoulded. In a modified classification scheme (i.e. one with intermediate plasticity for liquid limits between 35 and 50) the rock is a clay of intermediate plasticity with some low and rare high plasticities.

The plot of liquidity index versus depth included on Figure 2 shows that about one quarter of the samples have an insitu moisture content approximately equal to the plastic limit (i.e. liquidity index between  $\pm 0.1$ ) with half the samples below this level and the remaining quarter above.

## 5 UNDRAINED SHEAR STRENGTH

Triaxial undrained shear strength tests were completed on 220 samples, many of which were subjected to multistaged testing. The samples were not saturated prior to loading. To minimise the effect of incomplete saturation, we have used only the result of the first low cell pressure stage. A histogram of the test results is given on Figure 5 and the descriptive statistics for the test results in Table II.

TABLE II  
UNDRAINED SHEAR STRENGTH STATISTICS

Number of Tests	Mean kPa	Median kPa	Standard Deviation kPa	Minimum kPa	Maximum kPa
220	409	280	438	6	1,932

Reference to Figure 5 indicates that the distribution is highly non normal. Also the results fail goodness-of-fit tests for log-normality. Thus statistical methods based on assuming these distributions should be avoided. The geometric mean is 206 kPa with a multiplicative standard deviation of 3.82. The dashed line shows an exponential distribution fitted to the data. The hypothesis that the data is exponentially distribu-

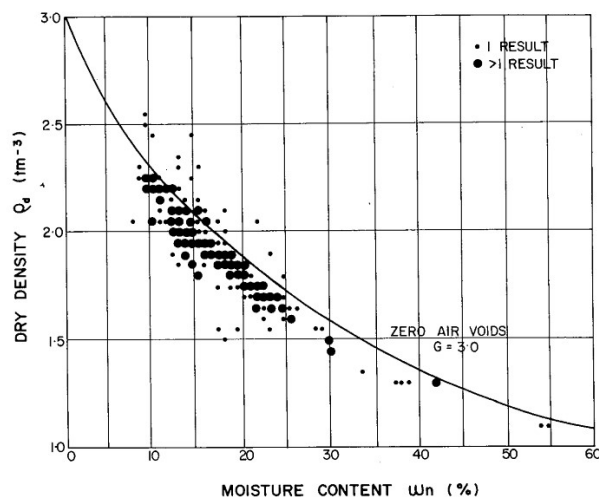


Figure 3 Moisture content versus dry density

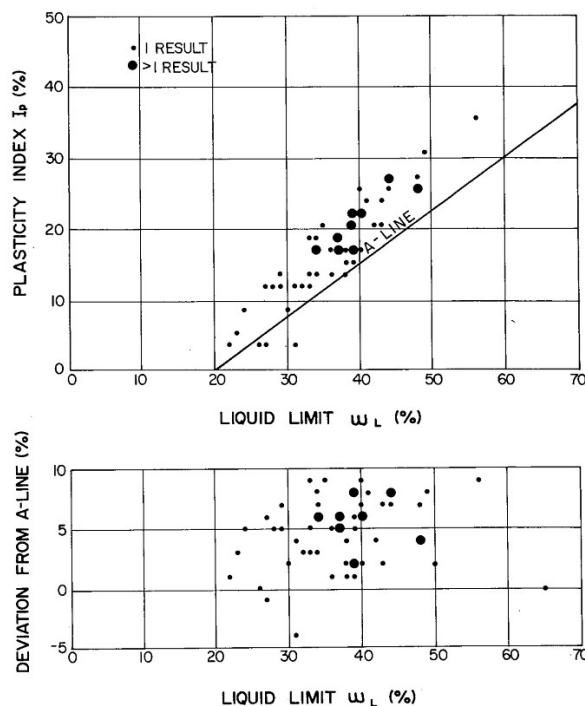


Figure 4 Atterberg limit test results

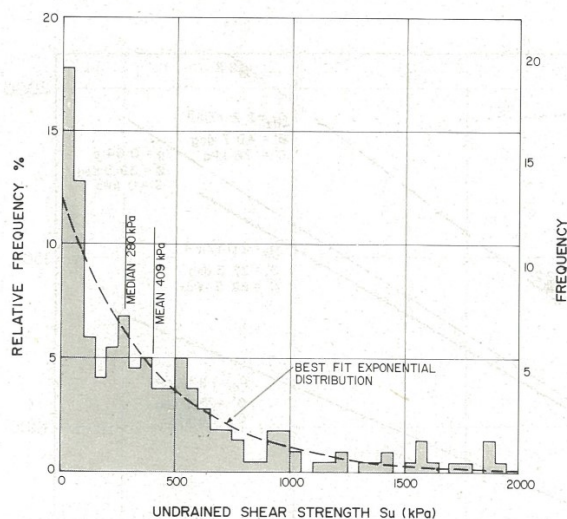


Figure 5 Histogram of undrained shear strength results

ted with a mean of 409 kPa was tested at a 95% confidence level by the Kolmogorov-Smirnov test and accepted.

The scatter of undrained shear strength ( $S_u$ ) with depth is plotted in Figure 2 and shows that very little relation exists between these two variables. Regression analysis indicates that at the most 20 percent of the variance of  $S_u$  can be explained by a knowledge of depth. In fact once the variation due to density (as discussed later) is removed, virtually no relationship exists between  $S_u$  and depth.

Further regression analysis indicated that dry density is the most significant predictive variable for undrained shear strength. The scatter of undrained shear strength with dry density is plotted on Figure 6. The relationship between  $S_u$  and  $\rho_d$  is:

$$S_u = 179 \exp(\rho_d) - 835 \text{ kPa} \quad (3)$$

The standard error for this relationship is 329 kPa and  $r$  squared is 0.438. Thus while the relationship is not strong, it can be useful to predict the average undrained shear strength for a given density. The 95% confidence limits for estimates of mean undrained shear strength determined from this regression line are also plotted on Figure 6 as are the confidence limits determined by usual statistical techniques applied to the test results alone. Note that this method (i.e. Student's method) assumes normality and, although normally considered robust, could be in error for the given data.

## 6 EFFECTIVE STRENGTH PARAMETERS

Two types of tests were conducted to determine the effective strength parameters of the mudstone, these were:

- o direct shear tests in a soil type shear box and
- o drained and undrained with pore pressure measurement triaxial tests.

All tests were single staged; twenty six stages were completed on the shear box and twenty one in the triaxial apparatus.

A least squares regression analysis on the results

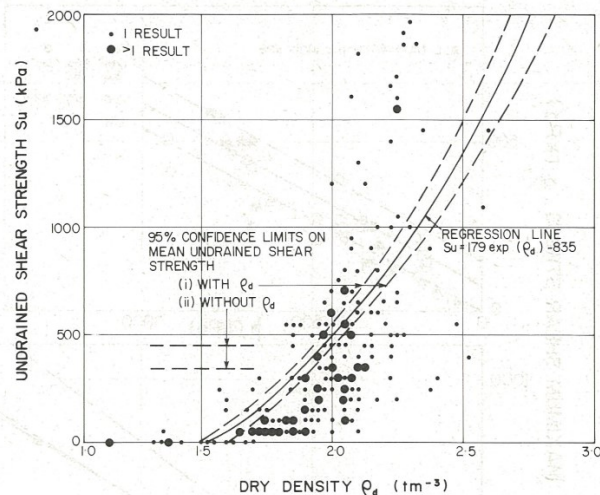


Figure 6 Scatter of undrained shear strength with dry density

of the tests performed in the shear box gave an effective cohesion ( $C'$ ) of approximately 100 kPa and an angle of friction ( $\phi'$ ) of 25 degrees. This  $\phi'$  was then used to map the normal stress ( $\sigma_n$ ) and failure shear stress ( $\tau_f$ ) pairs onto the  $p$ - $q$  plane. Subsequent analyses are not very dependent on the  $\phi'$  used in the mapping. The results for all the effective strength tests are presented in Figure 7. (Note that when a regression analysis was conducted with the cohesion fixed at zero, the best fit  $\phi'$  for the direct shear test results was 37.0 degrees and for the triaxial test results was 37.8 degrees - thus both suites of effective strength test results are spread about the same secant  $\phi'$ ).

The mapping resulted in  $p$ , $q$  data pairs for each stage of the effective strength testing programme including both the triaxial and direct shear testing; thus standard statistical techniques could be applied uniformly to the data from the two sources. Least squares regression analyses were completed on the data. By far the most significant regression computed for all the data points was:

$$q = 50.3 + (0.84 \rho_d - 1.09)p \text{ kPa} \quad (4)$$

with a standard error of estimate of 59 kPa and  $r$  squared of 0.979

This relationship implies that  $\phi'$  varies with  $\rho_d$  while the intercept on the  $q$  axis ( $q_0$ ) is constant; thus the variation in the cohesion ( $C'$ ) is due entirely to the variation in  $\phi'$  (because  $C' = q_0 / \cos \phi'$ ). The variation in  $C'$  and  $\phi'$  for different densities is shown in Table III.

TABLE III  
REGRESSION RESULTS FOR ALL EFFECTIVE STRENGTH DATA

Dry Density $\text{tm}^{-3}$	Cohesion kPa	Angle of Friction degrees
1.8	56	25
2.0	63	37
2.2	78	50

The solid lines on Figure 7 represent the regression lines for dry densities of 1.8 and 2.0  $\text{tm}^{-3}$ . The triangular data points should lie below the lowest (i.e.  $\rho_d = 1.8 \text{ tm}^{-3}$ ) solid line while

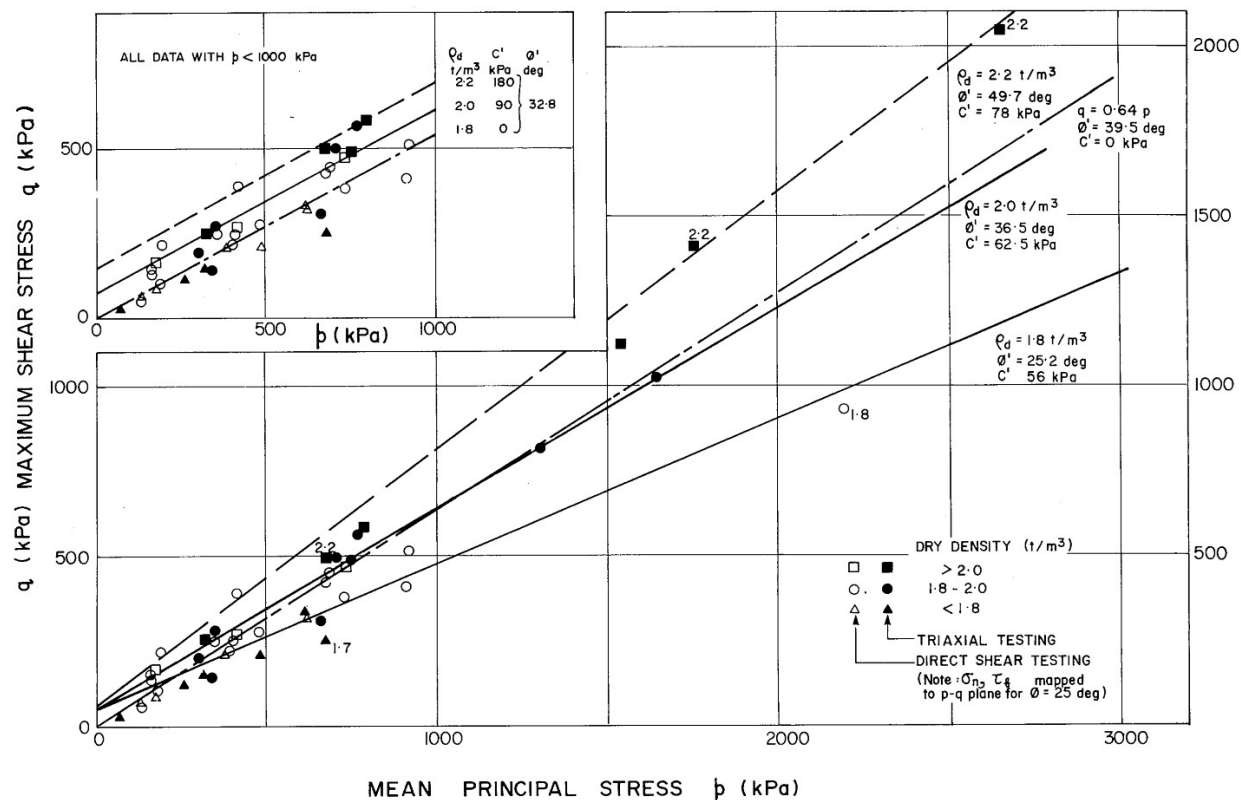


Figure 7 Results of effective strength testing

the square data points should lie above the upper (i.e.  $\rho_d = 2.0 \text{ t/m}^3$ ) solid line. The circular data points should lie between the lines. As can be seen, the proposed relationship fits the data well. The regression line for a dry density of  $2.2 \text{ t/m}^3$  is also plotted (as the uppermost line) and shows that the relationship also explains the extreme data points very well.

For reference and comparative purposes, the results of a simple linear least squares regression of  $q$  on  $p$  alone was also completed; this resulted in a small negative cohesion of  $-20 \text{ kPa}$  which is a common occurrence with this sort of analysis. The regression analysis was repeated with the cohesion set to zero and obtaining the best fit angle of friction. This approach is to be preferred to the approach commonly adopted in these cases of setting the cohesion to zero but using the angle of friction obtained from the analysis and thus not re-optimising  $\phi'$ . The regression resulted in the following relationship:

$$q = 0.636 p \quad \text{kPa} \quad (5)$$

with a standard error of estimate of  $121 \text{ kPa}$  and  $r$  squared of  $0.906$

This is equivalent to a cohesion of  $0 \text{ kPa}$  (as set in the analysis) and an angle of friction of  $39.7$  degrees. The phantom line in Figure 7 shows this relationship. It can be seen that there is much more spread about this regression line than about the surface represented by the dry density dependent relationship.

Further analyses were completed on the subset of test results with  $p$  less than  $1,000 \text{ kPa}$ , these analyses were completed for two reasons:

- o the stress range of interest is zero to  $1,000 \text{ kPa}$  and
- o to examine the effects of the high  $p, q$  points on the relationships derived.

The best fit regression is illustrated in the inset to Figure 7 and is:

$$q = (371 \rho_d - 668) + 0.54 p \quad \text{kPa} \quad (6)$$

for  $p < 1,000 \text{ kPa}$

with a standard error of estimate of  $50 \text{ kPa}$  and  $r$  squared of  $0.906$

This relationship is equivalent to an angle of friction of  $33$  degrees and a cohesion as shown in Table IV.

TABLE IV  
COHESION FOR DATA WITH  $p$  LESS THAN  $1000 \text{ kPa}$

Dry Density $\text{t/m}^3$	Cohesion $\text{kPa}$
1.8	1
2.0	90
2.2	178

Thus it appears that at low stress, the primary effect of an increase in density is to increase the cohesion; whereas for a large stress range, the effect is mainly on the angle of friction.

## 7 CONCLUSIONS

The data in this paper is presented primarily to document the properties of a particular soft rock. The several relationships derived are not viewed as



of any wide significance except in that they typify the type of relationships that would commonly be expected to hold for soft rock. They are not useful for predicting the strength insitu of the rock because little more is known about the independent variable (i.e.  $\rho_d$ ) than about the dependent variables. The very strong relationship between effective strength and  $\rho_d$  is cited because it confirms an often held opinion.

The methods of analyses presented in this paper would be of considerable advantage in a situation where some control was exercisable on the density of the material. This situation usually exists in the design of a dam embankment and the above relationships (determined for the subject soil) would enable the calculation of the cost-benefits of a change in the specified level of compaction.

The final point to be made is that even though there were over five times as many undrained shear strength tests performed as effective strength tests, the variation in  $S_u$  is far greater than in the effective strength parameters. It is often claimed that total stress stability analyses avoid the inherent uncertainty associated with estimating the location of the phreatic surface for use in an effective stress analysis; whilst this statement is correct, it is obvious that the uncertainty has been shifted into the determination of the strength parameters. The authors are of the opinion that such analyses are best completed using effective strength parameters, which are hopefully more accurately bound, and imprecise groundwater information. In this manner, the uncertainty is placed in the most natural place.

## 8 REFERENCES

ARNOLD, G.O., GRIFFIN, I.J and HODGE, C.C. (1979). Geology of the Ok Tedi and Southern Atbalmin, Geol. Survey of Papua New Guinea, Report 79/3.

CHUI, J.K. and JOHNSTON, I.W. (1983). The Uniaxial Properties of Melbourne Mudstone. Proc. 5th

International Congress on Rock Mechanics, Melbourne, pp. A209-A214.

EVERITT, P.R. and GOLDFINCH, R.W.S. (1974). The Shear Strength of Clay Gouges in the Sedimentary Rocks of Natal. Proc. 3rd International Conference on Rock Mechanics, Denver, pp. A101-A104.

JOHNSTON, I.W., WILLIAMS, A.F. and CHIU, H.K., (1980). Properties of Soft Rock Relevant to Socketed Pile Design. Proc. International Conference on Structural Foundations on Rock, Sydney, pp. 55-64.

MANDZIC, E. (1979). Generalisation of Factors Effecting the Uniaxial Strength of Rock Material. Proc. 4th International Conference on Rock Mechanics, Montreux, pp. 397-408.

MAYNE, P.W. (1980). Cam-Clay Predictions of Undrained Strength. Journal of the Geotechnical Division, Proc. A.S.C.E., Vol. 106, No. GT11.

ONODERA, F.T. and DUANGDEUN, P. (1981). Dependence of Mechanical Properties to the Texture and Water Content of Weak Rock. A case of the Late Tertiary Mudstone from the Mae Mo Lignite Mine, Northern Thailand. Proc. International Symposium on Weak Rock, Tokyo, pp. 327-332.

SAINT SIMON, P.G.R., SOLYMAR, Z.V. and THOMPSON, W.J. (1979). Damsite Investigation in Soft Rocks of Peace River Valley, Alberta. Proc. 4th International Conference on Rock Mechanics, Montreux, pp. 553-560.

SMORODINOV, M.I., MOTOVILOV, E.A. and VOLKOV, V.A. (1970). Determinations of Correlation Relationships Between Strength and Some Physical Characteristics of Rocks. Proc. 2nd International Conference on Rock Mechanics, Beograd, pp. 35-38.

SUN G. and ZHOU, R. (1983). The Structural Effect in the Mechanical Behaviour of Clay Shale. Proc. 5th International Conference on Rock Mechanics, Melbourne, pp. A153-156.